Electronic structure investigation of MAX-phases by soft x-ray emission spectroscopy

Martin Magnuson

Original Publication:

Martin Magnuson, Electronic structure investigation of MAX-phases by soft x-ray emission spectroscopy, 2007, *MRS Online Proceedings Library*, Volume 1023.
http://dx.doi.org/10.1557/PROC-1023-JJ09-01

MRS Proceedings, 1023, 1023-JJ09-01 doi:10.1557/PROC-1023-JJ09-01

Electronic Structure Investigation of MAX-phases by Soft X-ray Emission Spectroscopy

Martin Magnuson

Department of Physics, Uppsala University, P. O. Box 530, Uppsala, S-75121, Sweden

ABSTRACT

The electronic structure of nanolaminate Ti_2AlC and Ti_2AlN thin films, so-called MAX-phases, were investigated by soft X-ray emission spectroscopy. These nanolaminated carbide and nitride compounds represent a class of layered materials with a combination of properties from both metals and ceramics. The bulk-sensitive soft X-ray emission technique is particularly useful for detecting detailed electronic structure information about internal monolayers and interfaces. The Ti-Al bonding is manifested by a pronounced peak in the Ti *L*-emission of Ti_2AlC and Ti_2AlN that is not present in the binary TiC system. The spectral shape of Al *L*-emission in the MAX-phase is strongly modified in comparison to metallic Al. By replacing or partly exchanging C with N, a change of the electron population can be achieved causing a change of covalent bonding between the laminated layers, which enables control of the material properties.

INTRODUCTION

The important family of ternary carbide and nitride compounds, so-called $M_{n+1}AX_n$-phases is the subject of intense research [1]. Three different kinds of crystal structures (stoichiometries) are classified as 211 (n=1), 312 (n=2) and 413 (n=3) phases [2-4]. Here, the letter M denotes an early transition metal, A is an element in the groups III-V and X is either carbon or nitrogen. The MAX-phases exhibit a technologically important combination of metallic and ceramic properties, including high strength and toughness at high temperature, resistance to oxidation and thermal shock, exhibit high electrical and thermal conductivity [1], is environmentally friendly and relatively cheap to produce. The unique materials properties of the MAX-phases are related to the internal nanolaminated crystal structure, the choice of the three constituent elements, as well as the electronic structure and the chemical bonding between the intercalated atomic layers. For the 211 type of crystal structure, there are about 50 different ternary carbides and nitrides, among which Ti_2AlC and Ti_2AlN can be anticipated to be technologically useful. Sintered bulk MAX-compounds are useful in many technological high-temperature applications such as heating elements in ovens and construction parts of combustion engines. In other applications where tribological properties e.g., low-friction and wear resistance are important such as electrical switches, high quality thin film single-crystalline coatings of MAX-phases can be utilized.

In this paper, soft x-ray emission (SXE) spectroscopy was applied to probe the internal electronic structures of Ti_2AlC and Ti_2AlN in comparison to the binary compounds TiC and TiN. The photon-in-photon-out SXE spectroscopic technique is element selective and more bulk sensitive than electron-based techniques such as x-ray absorption and x-ray photoemission spectroscopy [5-7]. This makes it possible to obtain information about buried intercalated monolayers, chemical bonding and interfaces in complex compounds. The internal electronic structure of each constituent atomic element in a MAX-phase compound can be probed separately and provide elemental as well as chemical information about the partial electronic structure of the occupied valence band projected by the dipole transition selection rules to the core level of each element. Investigation of the electronic structure and chemical bonding aim to increase the understanding of its correlation to the physical properties of the studied materials. It is important that single crystal material is employed in order to understand and obtain the basic physical properties. The target of the research is to understand and systematize how the underlying electronic structure and chemical bonding affects the macroscopic properties.

EXPERIMENT

The SXE measurements were performed at the undulator beamline I511-3 at MAX II (MAX-lab National Laboratory, Lund University, Sweden), which includes a 49-pole undulator and a modified SX-700 plane grating monochromator [8]. The SXE spectra were recorded with a high-resolution Rowland-mount grazing-incidence grating spectrometer [9] with a two-dimensional detector. The Ti *L*, C *K* and N *K* SXE spectra were measured using a spherical grating with 1200 lines/mm of 5 m radius in the first order of diffraction. The Al *L* spectra were measured using a grating with 300 lines/mm, 3 m radius in the first order of diffraction. During the SXE measurements at the Ti *2p*, C *1s*, N *1s* and Al *2p* edges, the resolutions of the beamline monochromator were 1.6, 1.0, 0.75 and 0.3 eV, respectively. The Ti *L*, C *K*, N *K* and Al *L* SXE spectra were recorded with spectrometer resolutions 0.7, 0.2, 0.3 and 0.2 eV, respectively. The measurements were performed with a base pressure lower than 5×10^{-10} Torr. In order to minimize self-absorption effects [10], the angle of incidence was 20 degrees from the surface plane during the emission measurements. The x-ray photons were detected parallel to the polarization vector of the incoming beam in order to minimize elastic scattering. The deposition procedure of the epitaxially grown thin film coatings are described elsewhere [4,11].

RESULTS AND DISCUSSION

Figure 1 shows soft x-ray emission spectra of Ti_2AlC (full curves) and TiC (dotted curves) excited nonresonantly above the Ti *L* (top), C *K* (middle) and Al *L* edges (bottom). The excitation energies were 477 eV, 310 eV and 120 eV, respectively. For comparison, the spectra are normalized to unity and plotted on a common energy scale relative to the Fermi level (E_F) using the core level XPS binding energies of Ti_2AlC [4]. For Ti $2p_{1/2}$, C *1s* and Al $2p_{1/2}$, 460.3 eV, 281.9 eV and 72 eV binding energies were used, respectively.

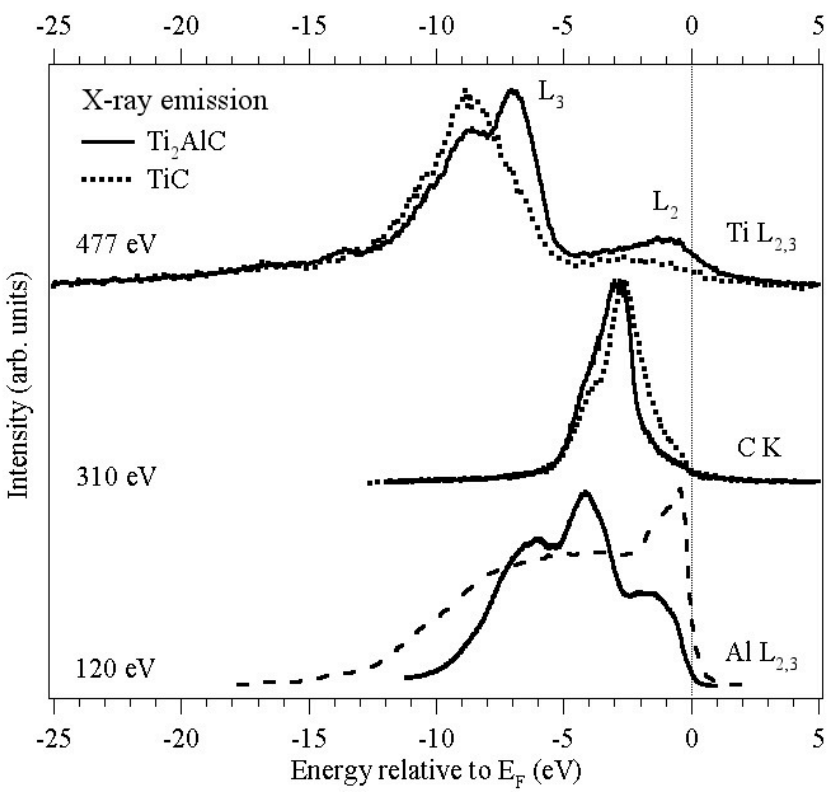

Figure 1: Soft X-ray emission spectra of Ti_2AlC and TiC.

In the Ti $L_{2,3}$ spectra at the top of Figure 1, the main L_3 and L_2 emission lines following the *3d,4s* –> $2p_{3/2,1/2}$ dipole transitions are clearly observed at -7 eV (-1 eV from the E_F when the Ti *2p* spin-orbit splitting is subtracted) and -1 eV. The intensity of the L_3 emission line is about 6 times larger than the L_2 intensity. This is due to the fact that the L_2 –> L_3M Coster-Kronig decay change the initial core hole population from the statistical one (2:1), preceding the SXE process [10]. The measured peak splitting due to the Ti *2p* spin-orbit interaction is 6.2 eV. Considering the L_3 region, the most significant difference between the two systems is the pronounced double peak in Ti_2AlC that does not exist in TiC. The peak splitting of the double peak is 1.5 eV.

In the C *K* spectra in the middle of Figure 1, the main peak is found at -2.6 eV and there are shoulders on both the low- and high-energy sides of the main peak at -4.2 eV and -1 eV. The high-energy shoulder is more pronounced in Ti_2AlC while the low-energy shoulder is more pronounced in TiC. The main peaks and the shoulders correspond to the occupied C *2p* orbitals hybridized with the Ti *3d* states of the valence band.

The Al $L_{2,3}$ spectrum of Ti_2AlC at the bottom of Figure 1 has the main peak at -4 eV dominated by *3s* –> $2p_{3/2,1/2}$ dipole transitions. Additional *3d* –> $2p_{3/2,1/2}$ transitions close to the E_F form the broad peak structure around -1.5 eV and participate in the Ti-Al bonding in Ti_2AlC. Al *3p* states dominate close to the E_F but only contribute indirectly to the Al *L* SXE spectrum. The spectral profile of Al in Ti_2AlC also differs substantially from the spectrum of pure Al metal (dashed curves), which has a sharp and dominating peak structure close to the E_F [12]. A similar spectral profile as in Al of Ti_2AlC has been observed in the metal aluminides [13].

Considering the Ti $L_{2,3}$ spectrum of Ti_2AlC, the main peak at -7 eV mainly originates from Ti *3d* - Al *3p* hybridization, an interpretation that is also consistent with bandstructure calculations [4,14]. The -7 eV peak is absent in TiC which instead is dominated by a carbide-type of peak at -8.5 eV due to Ti *3d* - C *2p* hybridization. The broad peak structure observed approximately at -

17 eV in both the Ti $L_{2,3}$ spectra of Ti_2AlC and TiC is not observed in Ti $L_{2,3}$ spectra of pure Ti [15]. The -17 eV structure can therefore be attributed to the influence of carbon due to Ti *3d* - C *2s* hybridization.

Figure 2 shows soft x-ray emission spectra of Ti_2AlN and TiN excited nonresonantly above the Ti *L* (top), N *K* (middle) and Al *L* edges (bottom). The excitation energies were 486 eV, 431 eV and 110 eV, respectively. For comparison, the spectra are normalized to unity and plotted on a common photon energy scale relative to the Fermi level (E_F) using the core level XPS binding energies of TiN [7]. In the Ti $L_{2,3}$ spectra at the top of Figure 2, the main L_3 and L_2 emission lines dominated by *3d* final states are observed at -11 eV and -1 eV. The intensity of the L_3 emission line is about 15 times larger than the L_2 intensity. The L_2 –> L_3M Coster-Kronig decay which change the initial core hole population from the statistical one (2:1) [10], preceding the SXE process is thus significantly stronger in the nitrides than for the carbides (Figure 1). In addition, a strong peak is observed at -7 eV in both Ti_2AlN and TiN. The Ti $L_{2,3}$ SXE spectra of Ti_2AlN and TiN are rather similar in shape. The difference is the intensity of the main peak at -11 eV that is about 23 % higher in TiN than in Ti_2AlN. This is consistent with the change of stoichiometry when going from TiN to Ti_2AlN, as the Ti content is constant while the N content decreases from 50% to 25%. Considering the L_3 region, the most significant difference to the carbides is the pronounced peak at -7 eV that is present in both Ti_2AlN and TiN.

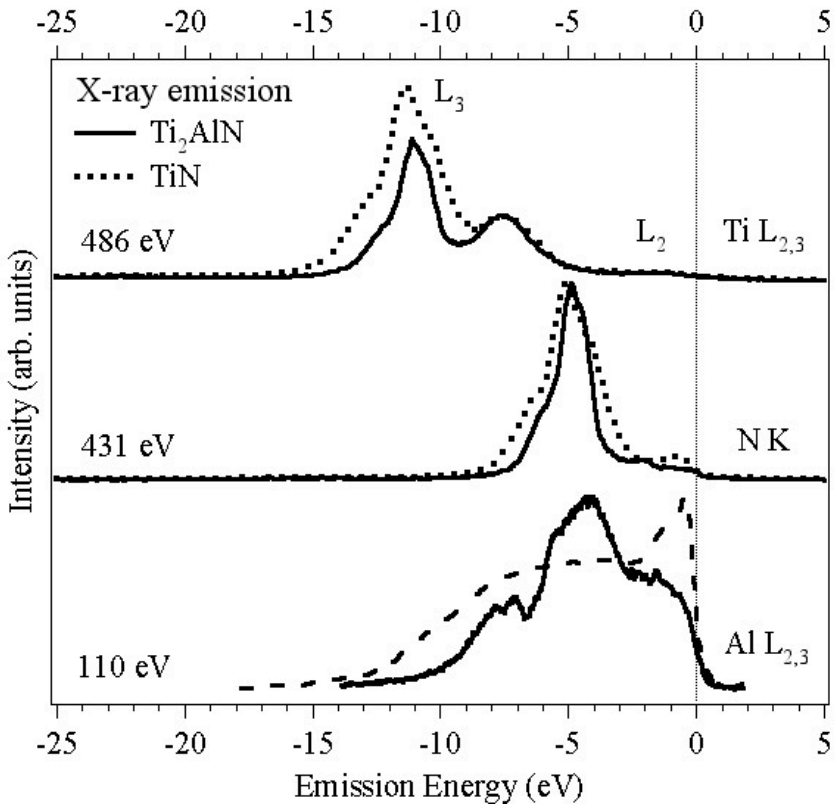

Figure 2: Soft X-ray emission spectra of Ti_2AlN and TiN.

In the N *K* spectra of Ti_2AlN and TiN in the middle of Figure 2, the main peak is found at -4.8 eV and there is a shoulder on the low-energy side at -6 eV.

The Al $L_{2,3}$ spectrum of Ti_2AlN at the bottom of Figure 2 has the main peak at -4.8 eV dominated by $3s$ –> $2p_{3/2,1/2}$ dipole transitions. Additional $3d$ –> $2p_{3/2,1/2}$ transitions close to the E_F form the

broad peak structure around -2 eV and participate in the Ti-Al bonding in Ti_2AlN. Al *3p* states dominate close to the E_F but only contribute indirectly to the Al *L* SXE spectrum. As in the case of Ti_2AlC, the spectral profile of Al in Ti_2AlN also differs substantially from the spectrum of pure Al metal (dashed curve), which has a sharp and dominating peak structure close to the E_F [12]. The sharp spectral structures at -7.0 and -7.7 eV below E_F in the Al $L_{2,3}$ SXE spectrum of Ti_2AlN can be attributed to the formation of hybridized Al *3s* states influenced by the orbital overlap with the Ti *3d*-orbitals in this energy region. A valley at -6.5 eV indicates withdrawal of charge in this region. A comparison between the spectral profiles of measured MAX-phases and electronic structure calculations including core-to-valence dipole transition matrix elements is presented elsewhere [4,11] yielding a qualitative agreement in the interpretation between experiment and theory.

CONCLUSIONS

Soft x-ray emission spectra of the MAX-phases Ti_2AlC and Ti_2AlN in comparison to TiC and TiN are presented. The most significant difference between the two compounds is a pronounced double peak in the Ti $L_{2,3}$ emission of Ti_2AlC. This feature originates from the Ti-Al bond region at -1 eV that is significantly closer to the Fermi level than the Ti-C bond regions at -2.5 eV and at -10 eV in Ti_2AlC and TiC. For Ti_2AlN, a strong peak in the Ti $L_{2,3}$ emission observed -4.8 eV below the Fermi level is due to intense Ti *3d* - N *2p* hybridization and covalent bonding while another peak observed -1 eV below the Fermi level is due to Ti *3d* states hybridized with Al *3p* states in a weaker covalent bonding. In addition, Ti *3d* - N *2s* hybridization is identified at -15 eV below the Fermi level as a weak spectral structure in the Ti $L_{2,3}$ emission. Analysis of the underlying electronic structure of these compounds provide increased understanding of the chemical trend of materials properties as more charge is introduced when replacing C in Ti_2AlC and TiC by N in Ti_2AlN and TiN. The Al $L_{2,3}$ x-ray emission spectral profiles of the intercalated Al monolayers in Ti_2AlC and Ti_2AlN are found to be very different in comparison to pure Al metal. The modified Al spectral profile is due to strong hybridization with the surrounding Ti and C atoms. By alloying or partly exchanging C with N atoms, the additional valence electron population and thus the modified chemical bonding scheme implies that the macroscopic material properties effectively can be tailored.

ACKNOWLEDGMENTS

The staff at MAX-lab, Lund, Sweden is acknowledged for experimental support and the Thin Film Physics Division at Linkoping University, Sweden is acknowledged for making the samples. This work was supported by the Swedish Research Council and the Goran Gustafsson Foundation.

REFERENCES

1. M. W. Barsoum; Prog. Solid State Chem. **28**, 201 (2000).
2. M. Magnuson, J. -P. Palmquist, M. Mattesini, S. Li, R. Ahuja, O. Eriksson, J. Emmerlich, O. Wilhelmsson, P. Eklund, H. Högberg, L. Hultman, U.Jansson; Phys. Rev. B **72**, 245101 (2005).
3. M. Magnuson, M. Mattesini, O. Wilhelmsson, J. Emmerlich, J. -P. Palmquist, S. Li, R. Ahuja, L. Hultman, O. Eriksson and U. Jansson, Phys. Rev. B. **74** 205102 (2006)
4. M. Magnuson, O. Wilhelmsson, J. -P. Palmquist, U. Jansson, M. Mattesini, S. Li, R. Ahuja and O. Eriksson, Phys. Rev. B. **74** 195108 (2006).
5. N. I. Medvedeva, D. L. Novikov, A. L. Ivanovsky, M. V. Kuznetsov and A. J. Freemena; Phys. Rev. B **58**, 16042 (1998).
6. S. E. Stoltz, H. I. Starnberg and M. W. Barsoum; J. Phys. and Chem. Of Solids; **64**, 2321 (2003).
7. S. Myhra, J. A. A. Crossley and M. W. Barsoum; J. Phys. Chem. Solids; **62**, 811 (2001).
8. R. Denecke, P. Vaterlein, M. Bassler, N. Wassdahl, S. Butorin, A. Nilsson, J.-E. Rubensson, J. Nordgren, N. Mårtensson and R. Nyholm; J. Electron Spectrosc. Relat. Phenom. **101-103**, 971, (1999).
9. J. Nordgren and R. Nyholm; Nucl. Instr. Methods **A246**, 242 (1986); J. Nordgren, G. Bray, S. Cramm, R. Nyholm, J.-E. Rubensson and N. Wassdahl; Rev. Sci. Instrum. **60**, 1690 (1989).
10. M. Magnuson, M. Mattesini, S. Li, C. Hoglund, M.Beckers, L. Hultman and O. Eriksson; Phys. Rev. B, in press (2007).
11. M. Magnuson, N. Wassdahl and J. Nordgren; Phys. Rev. B **56**, 12238 (1997).
12. D. L. Ederer, R. Schaefer, K.-L. Tsang, C. H. Zhang, T. A. Callcott and E. T. Arakawa; Phys. Rev. B **37**, 8594 (1988).
13. K. Ichikawa; J. Phys. Soc. Jpn. **37**, 377 (1994).
14. Y. Zhou, Z. Sun, X. Wang and S. Chen; J. Phys. Condens. Matter **13**, 10001 (2001).
15. E. Z. Kurmaev, A. L. Ankudinov, J. J. Rehr, L. D. Finkelstein, P. F. Karimov and A. Moewes; J. Elec. Spec. **148**, 1 (2005).